

## Article

# Transcriptomic Changes and *satP* Gene Function Analysis in *Pasteurella multocida* with Different Levels of Resistance to Enrofloxacin

Xue-Song Li <sup>1,2</sup>, Yu Qi <sup>1,2</sup>, Jun-Ze Xue <sup>1,2</sup>, Guan-Yi Xu <sup>1,2</sup>, Yu-Xuan Xu <sup>1,2</sup>, Xuan-Yu Li <sup>1,2</sup>, Inam Muhammad <sup>1,2</sup>, Ling-Cong Kong <sup>1,2,\*</sup> and Hong-Xia Ma <sup>1,2,3,4,\*</sup>

<sup>1</sup> Department of Veterinary Medicine, College of Animal Science and Technology, Jilin Agricultural University, Xincheng Street No. 2888, Changchun 130118, China

<sup>2</sup> The Key Laboratory of New Veterinary Drug Research and Development of Jilin Province, Jilin Agricultural University, Xincheng Street No. 2888, Changchun 130118, China

<sup>3</sup> College of Life Sciences, Jilin Agricultural University, Xincheng Street No. 2888, Changchun 130118, China

<sup>4</sup> The Engineering Research Center of Bioreactor and Drug Development, Ministry of Education, Jilin Agricultural University, Xincheng Street No. 2888, Changchun 130118, China

\* Correspondence: lingcong@jlau.edu.cn (L.-C.K.); mahongxia@jlau.edu.cn (H.-X.M.)

**Simple Summary:** *Pasteurella multocida* is a major pathogen of bovine respiratory disease, which is resistant to many of the commonly used antibiotics. We found that enrofloxacin has shown a high drug resistance in clinical treatment of *Pasteurella multocida* infection. In order to better understand the resistance mechanism of *Pasteurella multocida* to enrofloxacin, we isolated *PmS* and *PmR* strains with the same PFGE typing in vitro, and artificially induced *PmR* to obtain the highly resistant phenotype, *PmHR*. Then, transcriptome sequencing of clinically isolated sensitive strains, resistant and highly drug-resistant strains, treated with enrofloxacin at sub-inhibitory concentrations, were performed. The *satP* gene, of which the expression changed significantly with the increase in drug resistance, was screened. In order to further confirm the function of this gene, we constructed the deleted and complemented strains of *satP*, and further analyzed the function of the *satP* gene. After *satP* gene deletion, the resistance of *Pasteurella multocida* was obviously lower than that of wild-type strains in vitro, and the pathogenicity of *Pasteurella multocida* was reduced by about 400 times. We found that the *satP* gene is related to the tolerance and pathogenicity of *Pasteurella multocida*, and can be used as a target of enrofloxacin synergistic effect.



**Citation:** Li, X.-S.; Qi, Y.; Xue, J.-Z.; Xu, G.-Y.; Xu, Y.-X.; Li, X.-Y.; Muhammad, I.; Kong, L.-C.; Ma, H.-X. Transcriptomic Changes and *satP* Gene Function Analysis in *Pasteurella multocida* with Different Levels of Resistance to Enrofloxacin. *Vet. Sci.* **2023**, *10*, 257. <https://doi.org/10.3390/vetsci10040257>

Academic Editor: Karl Pedersen

Received: 15 February 2023

Revised: 22 March 2023

Accepted: 25 March 2023

Published: 28 March 2023



**Copyright:** © 2023 by the authors. Licensee MDPI, Basel, Switzerland. This article is an open access article distributed under the terms and conditions of the Creative Commons Attribution (CC BY) license (<https://creativecommons.org/licenses/by/4.0/>).

**Abstract:** *Pasteurella multocida* (*Pm*) is one of the major pathogens of bovine respiratory disease (BRD), which can develop drug resistance to many of the commonly used antibiotics. Our earlier research group found that with clinical use of enrofloxacin, *Pm* was more likely to develop drug resistance to enrofloxacin. In order to better understand the resistance mechanism of *Pm* to enrofloxacin, we isolated *PmS* and *PmR* strains with the same PFGE typing in vitro, and artificially induced *PmR* to obtain the highly resistant phenotype, *PmHR*. Then transcriptome sequencing of clinically isolated sensitive strains, resistant and highly drug-resistant strains, treated with enrofloxacin at sub-inhibitory concentrations, were performed. The *satP* gene, of which the expression changed significantly with the increase in drug resistance, was screened. In order to further confirm the function of this gene, we constructed a *satP* deletion ( $\Delta Pm$ ) strain using suicide vector plasmid pRE112, and constructed the *C-Pm* strain using pBBR1-MCS, and further analyzed the function of the *satP* gene. Through a continuously induced resistance test, it was found that the resistance rate of  $\Delta Pm$  was obviously lower than that of *Pm* in vitro. MDK<sub>99</sub>, agar diffusion and mutation frequency experiments showed significantly lower tolerance of  $\Delta Pm$  than the wild-type strains. The pathogenicity of  $\Delta Pm$  and *Pm* was measured by an acute pathogenicity test in mice, and it was found that the pathogenicity of  $\Delta Pm$  was reduced by about 400 times. Therefore, this study found that the *satP* gene was related to the tolerance and pathogenicity of *Pm*, and may be used as a target of enrofloxacin synergistic effect.

**Keywords:** bovine respiratory disease; *Pasteurella multocida*; drug resistance; antibiotic tolerance; *satP*

## 1. Introduction

*Pasteurella multocida* (*Pm*) is a Gram-negative bacterium implicated in multi-host infections. Strains of their species are currently classified into type A, type B, type D, type E and type F serogroups [1,2]. *Pm* is one of the primary pathogens of bovine respiratory disease (BRD) in Asia, Middle East, Africa and Europe [3–5]. At present, the infection of cattle with *Pm* leads to tremendous economic losses for the cattle industry due to increased mortalities and high treatment costs [6]. The treatment of BRD mainly depends on antibiotics, and penicillin has often been used as the drug of choice for the last few decades [7,8]. However, due to the irrational use of antibiotics in clinical treatment, it has been observed that the drug resistance rate of  $\beta$ -lactams, macrolides and tetracyclines has increased in recent years [9–12]. Irrational use of antibiotics to prevent the threat of BRD increases the rate of *Pm* resistance [13].

Fluoroquinolones are one of the main therapeutic drugs for *Pm* infections in animals [12]. Enrofloxacin has a good therapeutic effect on nasal, upper respiratory and lung infections caused by *Pm* infection in animals [14–16]. Unfortunately, *Pm* has recently been reported to possess acquired fluoroquinolone resistance mechanisms [17]. Among them, variation of DNA gyrase or topoisomerase IV, bacterial cell membrane permeability and bacterial active efflux mechanisms are the most common. DNA gyrase is a tetramer composed of GyrA and GyrB proteins, and topoisomerase VI is a tetramer composed of ParC and ParE proteins [18]. Mutation of any of these four proteins may cause drug resistance to fluoroquinolones. In *Pm*, *gyrA* gene mutation often leads to the structural change of DNA helicase, which leads to drug resistance. Within the *gyrA* gene, quinolone-resistant determining region (QRDR) is closely associated with drug resistance [19]. Mutation in this region can cause drug resistance. The specific positions of proteins encoded by this region are different across different strains. For example, they correspond to Gly–Asp94 in *Mycobacterium tuberculosis*, Ala67–Gln106 in *Escherichia coli* and Arg88Ile in *Pm*. Detection of QRDR gene mutation has been a hot issue in the early study of fluoroquinolone resistance [20]. Our previous results indicated that *Pm* is extremely resistant to fluoroquinolones in vivo and in vitro, and the mechanism is mainly mediated through target mutation in *gyrA* and *parC* [21]. The variation of DNA gyrase or topoisomerase VI is the main cause of bacterial resistance to fluoroquinolones.

The bacterial cell membrane is a highly selective permeable barrier. There are some special proteins in the outer membrane of bacteria, which are called outer membrane proteins (OMPs). OMPs account for about half of the cell wall in Gram-negative bacteria. The OMPs have the functions of antibiotic, iron transport, host adhesion and maintenance of membrane integrity [22]. At present, it is clear that OmpF, TolC and OmpX are related to fluoroquinolone resistance [23]. Simultaneously, there is an energy-dependent protein efflux pump in the inner membrane of *Pm* which can discharge drugs, resulting in drug resistance [24]. The efflux of fluoroquinolones in *Pm* is mainly related to the survival–nodulation–cell division (RND) family, which includes the transporters of calcium, cobalt and nickel [25]. Among Gram-negative bacteria, the AcrAB–TolC system is the main active efflux pump related to fluoroquinolones. The active efflux pump and the change of bacterial outer membrane permeability play an important role in multidrug resistance, and attention has been paid to this by researchers [26].

However, the development of antimicrobial resistance is a complicated multifactorial process, and related studies have shown that the formation of drug resistance also depends on tolerance factors [27,28]. Antibiotic tolerance is the ability of antibiotic-sensitive bacteria at the gene level to survive under the influence of antibiotic treatment concentration, which plays a key role in the process of bacterial infection. Antibiotic tolerance is involved in chronic and recurrent infections [29]. Thus, some genes, such as *recA*, are essential for increased tolerance to antibiotic treatment by enhancing repair of DNA damage that occurs directly from antibiotic-induced DNA damage. Relevant studies have confirmed that

amino acid mutations are related to the generation of tolerance [30,31]. Frequent use of antibiotics can enhance the antibiotic resistance of *Pm* [32]. Due to the importance of tolerance, there is a crucial need to identify new drug targets. Mechanistically, *Pm* tolerance to fluoroquinolones and the main targets for mediating tolerance have not been reported. To determine whether the resistance mechanism of *Pm* is caused by tolerance, it is crucial to work on a new tolerance mechanism and identify targets that can inhibit drug resistance.

## 2. Materials and Methods

### 2.1. Antibiotics, Culture Media, Bacterial Strains and Growth Conditions

The clinical *PmS* (*Pasteurella multocida* sensitive to ENR) and *PmR* (*Pasteurella multocida* resistant to ENR) were isolated from the lungs of dead cattle that have suffered from BRD in Shuangyang City, Jilin Province. The highly resistant strain (*PmHR* MIC of ENR is 64 µg/mL) was obtained according to the methods reported in previous studies [21]. The *PmS*, *PmR* and *PmHR* had the same molecular type after PFGE typing (previous research of our group) [8]. *Pm* was cultured on a brain–heart infusion (BHI) medium. Commercial antibiotics were purchased from Sigma-Aldrich Company. According to CLSI regulations, 20,480 µg/mL storage solution was prepared and frozen at −20 °C for later use. Growth was monitored by measuring the OD<sub>600</sub> of the liquid cultures using a Biophotometer (Nanodrop2000, Thermo, Thermo Fisher Scientific, Waltham, MA, USA).

### 2.2. Determination of the MIC of Fluoroquinolones

The minimum inhibitory concentration (MIC) was established by broth microdilution and two-fold agar dilution, as recommended by the Clinical and Laboratory Standard Institute guidelines in VET01-A4. The MICs of ciprofloxacin and enrofloxacin were tested in the range of 0.03 to 512 µg/mL. The *Pm* cells were inoculated into BHI media and incubated for 24h at 37 °C. Then, cells were harvested and washed three times with PBS. Each strain was inoculated at a density of 10<sup>5</sup> CFU/mL in BHI containing 0.03 to 512 µg/mL of ciprofloxacin and enrofloxacin, and grown for 24 h at 37 °C. The breakpoints used for fluoroquinolone were adopted from the CLSI document, VET01-A4. *Escherichia coli* ATCC25922 was used as a quality control strain.

### 2.3. Amplification and Sequencing of the QRDR Genes

Fluoroquinolone QRDR targets, *gyrA*, *gyrB*, *parC* and *parE* genes, were amplified by polymerase chain reaction (PCR) and compared using the *gyrA*-F (5'-CCTTATCGTAAATCCGCTCGTA-3'), *gyrA*-R (5'-CGCAGGGACTTTGGTTGG-3'), *gyrB*-F (5'-GAAATGACCCGCCGTA-3'), *gyrB*-R (5'-CTTGCCCTTCTTCACTTTGTA-3'), *parC*-F (5'-TACGAAGGCATTGACAAAC-3'), *parC*-R (5'-CCACTGTCCCTTGCCCTA-3'), *parE*-F (5'-AATACGGTAAAGCGGTGGC-3') and *parE*-R (5'-GGATTCTGCTGGCGGTTTC-3') primers [10]. Amplified PCR products (312 bp, 456 bp, 421 bp and 331 bp) were cloned into the pMD18-T (from TaKaRa, TaKaRa Biotechnology (Dalian) Co., Ltd., Dalian, China) easy vector via TA cloning and sequenced for identification of mutation positions.

### 2.4. RNA Extraction, Library Construction, and Sequencing

The cells were grown to an exponential phase (OD<sub>600</sub> = 0.5) and treated with ENR (sub-inhibitory concentration) over a period of 15 min. Total RNA extraction of *PmS*, *PmR* and *PmHR* was performed using an RNAiso Pure RNA Isolation Kit (TaKaRa, TaKaRa Biotechnology (Dalian) Co., Ltd., China), according to the manufacturer's instruction. The quality and quantity of RNA was assessed, and the library construction and sequencing were performed at Biomarker Technology (Beijing, China) using the Illumina HiSeq 2500 platform. The genome sequence and annotation information of *Pm* were obtained from the NCBI database (Accession No. NC\_014259.1). Quality-filtered reads were aligned to the reference genome sequence, using the CLC Genomics Workbench 4.0 (CLC Bio, Qiagen, Dusseldorf, GER).

To identify DEGs (differential expression genes) among the three different samples, the expression level for each transcript was calculated using the fragments of RPKM (read per kilo base per million mapped reads) method. edgeR (<https://bioconductor.org/packages/release/bioc/html/edgeR.html>, accessed on 11 November 2021) was used for differential expression analysis. The DEGs between the two samples were selected using the following criteria: (i) the logarithmic of fold-change should be greater than 2 and the false discovery rate (FDR) should be less than 0.05. To understand the functions of the differentially expressed gene, GO functional enrichment and KEGG pathway analyses were carried out by Goatools (<https://github.com/tanghaibao/Goatools>, accessed on 27 November 2021) and KOBAS (<http://kobas.cbi.pku.edu.cn/home.do>, accessed on 27 November 2021), respectively. DEGs were significantly enriched in terms of GO and metabolic pathways when their Bonferroni-corrected p-value was less than 0.05. Then, with the increase in drug resistance, differentially expressed genes were screened.

### 2.5. Quantitative Reverse Transcription PCR (RT-qPCR) Analysis

Expression of *satP*, *focA*, *napF*, *glgP* and *napD* genes was evaluated by qPCR at the mRNA level. The cells were grown to an exponential phase ( $OD_{600} = 0.5$ ) and treated with ENR (sub-inhibitory concentration) over a period of 15 min. Total RNA extraction of *PmS*, *PmR* and *PmHR* was performed using an RNAiso Pure RNA Isolation Kit (TaKaRa), according to the manufacturer's instruction, and was reverse-transcribed to cDNA. The real-time PCR process was performed on the Applied Biosystems 7500 Real-Time PCR System (ABI, state abbr., USA). The primers of *satP*-F (CGCCAAAAGCAAACGCCATACC) and *satP*-R (TACGCCAATCCGGGTCCATTAGG) were designed. The specificity of the qRT-PCR results was confirmed by agarose gel and melting curve analysis, and the data were analyzed by the Applied Biosystems™ 7500 software. All qPCR reactions were performed with six replicates.

### 2.6. Construction *satP* of the Deletion Strains and the Complemented Strains

The *satP* gene knockout was conducted with the suicide vector, pRE112. Briefly, the genome of the strain to be knocked out was amplified by PCR using UP-F/R and DOWN-F/R primers (Supplementary Table S1), respectively, to obtain the upstream and downstream regions of the *satP* gene. Then, the PCR products were mixed as the template for the next overlapping PCR, and UP-F and DOWN-R were used as primers to amplify the template. Finally, the amplified PCR product (1673 bp) was cloned into the PRE112 vector, and no base mutation was identified by sequencing. Then, the plasmid pRE112-*satP* was successively transformed into *DH5 $\alpha$* - $\lambda$ pir and *E. coli* WM3064. The single colony was inoculated into 5 mL BHI broth, then inoculated into the BHI agar medium containing 10% sucrose, and cultured overnight at 37 °C. The recombinant strain without the *satP* gene and pRE112 plasmid was screened (thus creating the *satP* mutant of the  $\Delta PmS$ ,  $\Delta PmR$  and  $\Delta PmHR$  deletion strains). The complemented strain, *CPmS*, was constructed with the expression plasmids pBBR1-MCS, by homologous recombination.

### 2.7. Tolerance of Wild-Type and *satP* Mutant

Tolerance was determined according to Westfall's and Cirz's method [33,34]. The tolerance of enrofloxacin was detected by micro broth dilution method and (MDK<sub>99</sub>) test (the minimum duration for killing 99% of cells), respectively. In short, wild-type strains, deletion strains and complemented strains were cultured to  $OD_{600} = 0.5$  and colonies were counted. The bacterial solution was diluted to a final concentration of  $10^6$  CFU/mL according to the counting results. The final concentration of ENR with MIC was added to the culture medium, 50  $\mu$ L per hour was taken, and the colonies were counted after dilution. The line diagram of MDK<sub>99</sub> was made with the number of colonies as abscissa and time as ordinate. The experiment was set up three times. At the same time, 200  $\mu$ L per hour was added into a 96-well plate, diluted 10 times continuously, and participated in dilution 5 times. The diluted bacterial solution was inoculated on the BHI solid plate

through a multi-point inoculator. The growth of the colonies was observed the next day and the results recorded.

### 2.8. Animal Studies

Female BALB/c mice, aged 6–8 weeks (18–20 g), were obtained from the Animal Experimental Center of Jilin University (Changchun, China). All experiments were carried out under the Regulations of Jilin Laboratory Animal Management Committee of Jilin Province. The license number of experimental animals was JLAU20210423001, which is certified by Jilin Science and Technology Association.

#### 2.8.1. Pathogenicity Test in Mice

Twenty-five mice, both male and female, were randomly divided into five groups, with five mice in each group. After 3 days of adaptive feeding, the mice were reared without food and water for 12 h, and then *PmS* with bacterial counts of  $10^8$ ,  $10^7$ ,  $10^6$ ,  $10^5$  and  $10^4$  CFU/mL were intraperitoneally injected in mice. The condition of the mice was observed within seven days and the doses leading to the death of the mice were recorded. The LD<sub>50</sub> of the *PmS* strain was calculated by the Bliss method. The LD<sub>50</sub> of the  $\Delta$ *PmS* and *CPmS* strains was determined by the same method as that of the *PmS* strain.

Fifty mice, half male and half female, were randomly divided into five groups, with 10 mice in each group. After adaptive feeding for 3 days, the mice were reared without food and water for 12 h. According to the results of the preliminary experiment, each strain of bovine type A *Pm* was diluted to different concentrations, and each strain was set with five concentration gradients. The infection was carried out by intraperitoneal injection, and each mouse was infected with 100  $\mu$ L. The control group was injected with the same dose of sterile PBS buffer. After 48 h of observation, the death rate was noted. The LD<sub>50</sub> of each strain in the mice was calculated by the Bliss method, using the SPSS 26.0 software.

#### 2.8.2. Acute Pathogenicity Protection Test in Mice

Sixty mice, half male and half female, were randomly divided into six groups, with 10 mice in each group. After 3 days of adaptive feeding, the mice were kept without food and water for 12 h. The bacterial solution was centrifuged to remove the culture medium, then resuspended with normal saline, and the mice were injected with twice the concentration of LD<sub>50</sub>. The first and second groups were injected with *PmS* bacterial solution, the third and fourth groups were injected with  $\Delta$ *PmS* bacterial solution, and the fifth and sixth groups were injected with the *CPmS* bacterial solution.

One hour after bacterial injection, mice in the first, third and fifth groups were intramuscularly injected with a 100  $\mu$ L of ENR (2.5 mg/kg body weight) twice a day. The second and the fourth groups were injected with the same dose of normal saline intramuscular, and the survival conditions of the mice in each group were observed and recorded, and plotted by the Prism software, according to the previously reported methods [34,35].

## 3. Results

### 3.1. Selection of Fluoroquinolone-Resistant Mutants

Two strains (*PmS* and *PmR*) with the same molecular typing and different fluoroquinolone resistance phenotypes were isolated by 16S rRNA and PFGE (Supplementary Figure S1). A highly drug-resistant strain, *PmHR*, was obtained by in vitro fluoroquinolone induction, using *PmS* as the parental strain. By detecting the QRDR region, we found that *PmS* had no QRDR mutation, and *PmR* and *PmHR* had three identical QRDR mutations. (Table 1). It was noteworthy that the mutations in the *gyrA*, *gyrB* and *parC* genes of the highly resistant strain, *PmHR*, were the same as those of the resistant strain, *PmR*, which indicates that the difference in enrofloxacin resistance level was not due to QRDR mutations, and may have other forms of drug resistance mechanism.

**Table 1.** QRDR mutation genotypes and fluoroquinolone MICs for *PmS*, *PmR* and *PmHR*.

Strains	MIC Range ( $\mu\text{g/mL}$ )				Substitution in			
	CIP	ENR	ENR + CCCP	ENR + Verapamil	GyrA	GyrB	ParC	ParE
<i>PmS</i>	0.25	0.25	0.125	0.125	-	-	-	-
<i>PmR</i>	4	4	2	2	Arg88Ile	Ser467Phe	Glu84Lys	-
<i>PmHR</i>	64	64	64	64	Arg88Ile	Ser467Phe	Glu84Lys	-

The parent strain and mutant-derived strains were tested for carbonyl cyanide 3-chlorophenylhydrazone (CCCP)- and verapamil-sensitive efflux. The MICs of ENR were determined using the agar dilution method in the presence and absence of CCCP (4  $\mu\text{g/mL}$ , MIC/2) and verapamil (8  $\mu\text{g/mL}$ , MIC/2). These results indicated that the efflux pump genes did not play any role in the quinolone resistance of *Pm* mutants selected in vitro. The characteristic features of the three lineages are described in Table 1. We speculated that *PmHR* might be tolerant to ENR, and tolerance mechanisms should be investigated in future studies.

### 3.2. Transcriptional Profiling of *PmS*, *PmR* and *PmHR* by RNA Sequencing

In order to search for genes that played an important role in the formation of fluoroquinolone resistance in *Pm*, we sequenced the transcriptome of three strains under the sub-inhibitory concentration of ENR (Supplementary Table S2). The results showed that more than 97% of the reads can be mapped to the reference genome sequence (GenBank: 8172276). Raw read data were sequenced and filtered for further analysis, yielding approximately 1.76–2.15 billion clean reads. The average length of the reads for *PmS*, *PmR* and *PmHR* was 300bp, and their GC content was 42.77%, 43.17% and 42.35%, respectively, indicating successful sequencing of the *Pm* with different levels of ENR resistance (Supplementary Table S3).

In total, 14,055,756 clean reads were detected. Based on the FDR threshold  $\leq 0.05$  and  $|\log_2 \text{fold-change (FC)}| > 1$ , a total of 1,499 significant DEGs were identified. Simply put, compared with *PmS*, *PmR* has 144 up-regulated and 292 down-regulated genes. Compared with *PmS*, 181 genes were up-regulated and 382 genes were down-regulated in *PmHR*. Compared with *PmR*, 104 genes were up-regulated and 172 genes were down-regulated in *PmHR* (Supplementary Figures S2 and S3). The GO enrichment analysis and KEGG pathways were performed for DEGs. Enrichment analysis revealed significant changes in 19 GO biology processes, among which, seven biology processes were relating biological process, seven biology processes were relating cellular components and five biology processes were related to molecular function. These processes involve the intrinsic components and compositions of cell membranes, intracellular organelles, adhesion proteins and membrane-protein-related pathways. (Supplementary Figure S4). On the other hand, the top 20 of KEGG pathways were annotated. We annotated 650 DEGs and enriched them into 215 metabolic pathways. We further screened the enriched metabolic pathways, and categorized them into metabolic pathways such as antigen presentation and processing, cell adhesion, phagocytosis and cell killing and virulence. Among them, we found that antigen presentation and processing enriched DEGs were the most common. (Supplementary Figure S5 and Table S4).

Furthermore, in order to find the difference between *PmR* and *PmHR*, significantly expressed genes were screened with the improvement of drug resistance, and the *satP* (gene 1687), *focA*, *napF*, *glgP* and *napD* genes were significantly up-regulated (Table S5). As the most significantly expressed gene, the *satP* gene is mainly involved in encoding intimal proteins. By analyzing the expression of *satP*, we found that the expression of *satP* in the *PmR* group was 17 times higher than that in the *PmS* group, and the expression of *satP* in the *PmHR* group was 20 times higher than that in the *PmS* group (Figure 1A,B).

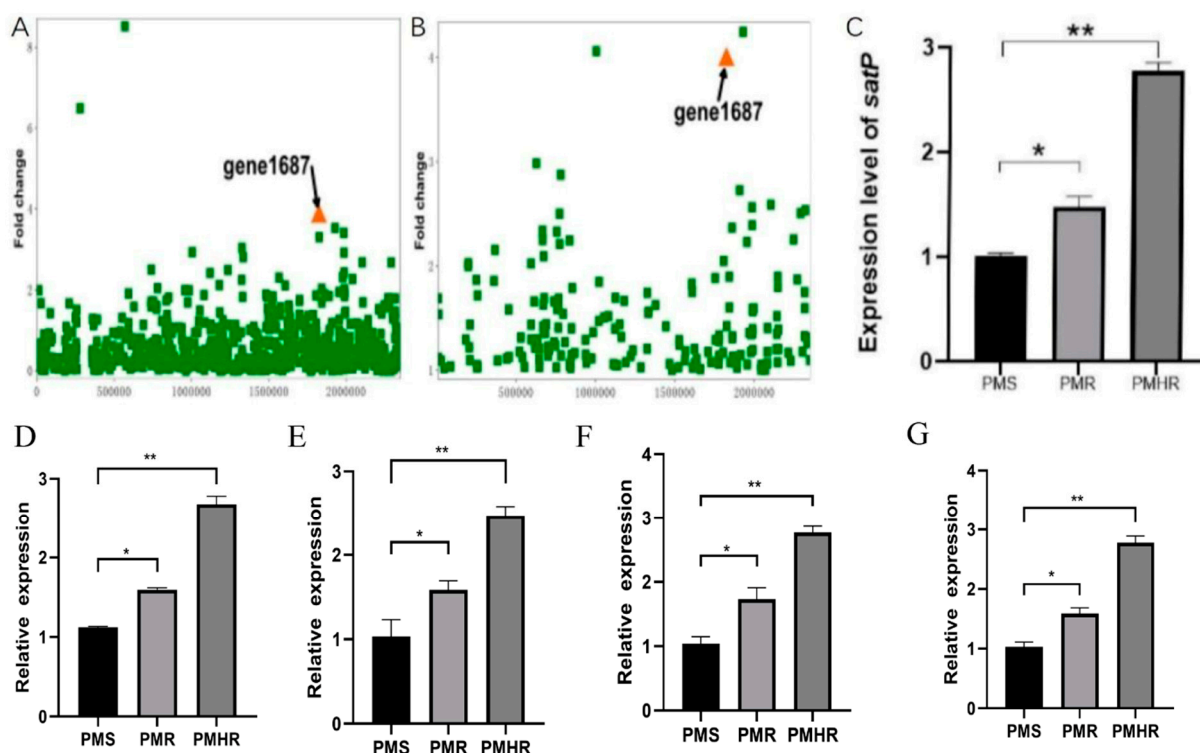


**Figure 1.** Characterization and verification of differentially expressed genes. (A) Differentially expressed gene analysis of resistance groups (*PmS* vs. *PmR*). (B) Differentially expressed gene analysis of resistance groups (*PmS* vs. *PmHR*). (C) *satP*, (D) *focA*, (E) *napF*, (F) *glgP* and (G) *napD* gene expression level verification using qRT-PCR. (All data are expressed as the mean  $\pm$  SD.  $n = 3$ . \*\*  $p < 0.01$  vs., \*  $p < 0.05$  vs. control group).

The qRT-PCR analysis was performed to validate the expression of *satP*, *focA*, *napF*, *glgP* and *napD* in *Pm* with different levels of drug resistance. As shown in Figure 1C–G, qRT-PCR results of *satP* agreed with the FPKM data. At the same time, the relative expression of *satP* in the *PmR* group was significantly higher than in the *PmS* group, and in the *PmHR* group significantly higher than in the *PmR* group. The expression level of *satP* gene was in accordance with the trend of drug resistance.

### 3.3. Construction and Detection of *satP* Strains

The knockout of *satP* in *PmS*, *PmR* and *PmHR* was conducted with the suicide vector pRE112. To determine whether  $\Delta PmS$ ,  $\Delta PmR$ ,  $\Delta PmHR$  and *CPmS* were successfully constructed, hereditary stability, PCR detection and qRT-PCR were performed. PCR showed that the *satP* deletion strains were 700bp less than that of the wild-type strain and *CPmS*. Real-time qRT-PCR showed that no signal of the *satP* gene was detected from the deletion strains. Genetic stability showed that  $\Delta PmS$ ,  $\Delta PmR$ ,  $\Delta PmHR$  and *CPmS* were successfully constructed. The deletion of *satP* did not affect the MIC and growth of the strains (Figure 2A–D).

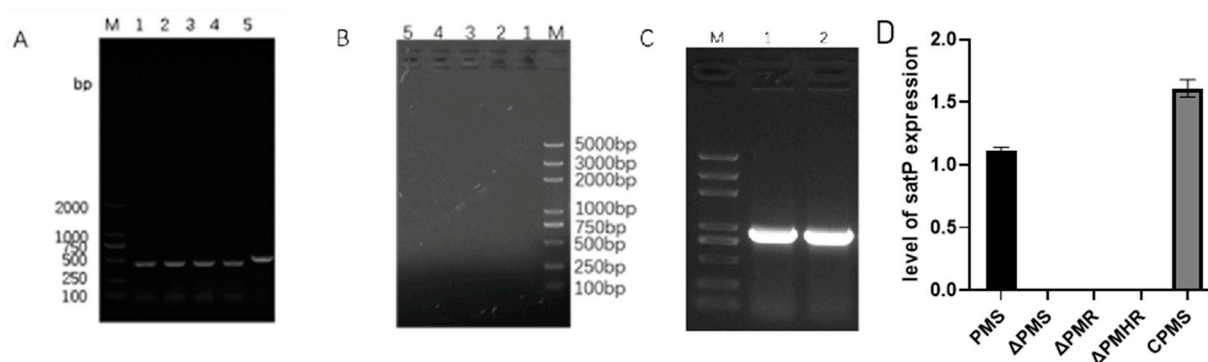


**Figure 2.** (A) Confirmation that the deletion of the *satP* strains were genetically stable beyond 40 generations by PCR. M: DL 2000 Marker; 1–4, deletions strain *satP*; 5, wild-type strain. (B) The genetic stability of *satP*-deficient strains over 40 generations was verified by pRE112 primers. M: 2000 plus DNA Marker; 1–4, deletions strain *satP*; 5, wild-type strain. (C) Confirmation that the *CPmS* was genetically stable beyond 40 generations by PCR. M, 2K plus DNA Marker; 1, wild-type strain; 2, *CPm*. (All data are expressed as the mean  $\pm$  SD.  $n = 3$ ). (D) The expression level of the *satP* gene in the wild-type strain, deletion strains and *CPmS*.

We found that when the *satP* gene was deleted,  $\Delta PmS$ ,  $\Delta PmR$  and  $\Delta PmHR$  had no QRDR mutation compared with those without deletion (Table 2). The MIC of ENR was determined by the agar dilution method in the presence and absence of CCCP (4 g/mL, MIC/2) and verapamil (8 g/mL, MIC/2). The results showed that the function of the efflux pump had no effect on the phenotype of *Pm* to ENR.

**Table 2.** QRDR mutation genotypes and fluoroquinolone MICs for  $\Delta PmS$ ,  $\Delta PmR$  and  $\Delta PmHR$ .

Strains	MIC Range ( $\mu\text{g/mL}$ )				Substitution in			
	CIP	ENR	ENR + CCCP	ENR + Verapamil	GyrA	GyrB	ParC	ParE
$\Delta PmS$	0.25	0.25	0.125	0.125	-	-	-	-
$\Delta PmR$	2	2	2	2	Arg88Ile	Ser467Phe	Glu84Lys	-
$\Delta PmHR$	64	64	64	64	Arg88Ile	Ser467Phe	Glu84Lys	-

### 3.4. Effect of *satP* Deletion on Drug Resistance Formation

To verify the effect of the *satP* gene on ENR resistance of *Pm*, an in vitro method of inducing drug resistance was used to detect the development time of drug resistance of the gene deletion strain, wild-type strain and replenishment strain. The results showed that in generation 1–5, the drug resistance of *PmS* was the same as that of the  $\Delta PmS$  and the *CPmS*, with an MIC of 0.5  $\mu\text{g/mL}$ . The drug resistance formation time of sensitive strains and gene deletion strains was different in generation 5–10. The resistance of *PmS* and the *CPmS* developed rapidly, with an MIC of 64  $\mu\text{g/mL}$  in the 10th generation. While the drug resistance of  $\Delta PmS$  developed slowly, and the MIC was 16  $\mu\text{g/mL}$  in the 10th generation (Figure 3A).

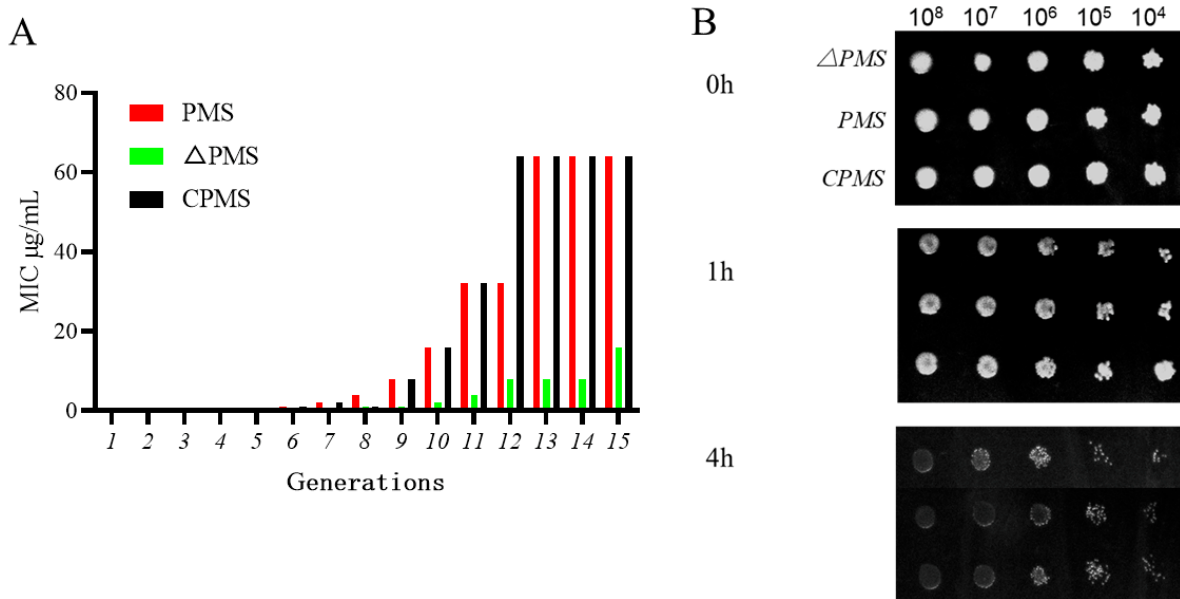


**Figure 3.** Effect of *satP* deletion on drug resistance formation and tolerance formation. (A) Development time of fluoroquinolone resistance of *PmS*,  $\Delta PmS$  and *CPmS*, induced by sub-inhibitory concentrations of enrofloxacin. (B) Tolerance test of  $\Delta PmS$  to enrofloxacin microdilution method.

3.5. Effect of  $\Delta PmS$  on Drug Tolerance Formation

The results showed that in  $10\times MIC$  enrofloxacin treatment, the killing effect of the  $\Delta PmS$  was faster than the *PmS* and *CPmS*, and the tolerance of the *satP* gene deletion strains to ENR was obviously weakened. The results of mutation frequency showed that the mutation frequency of the deletion strains decreased significantly (Figure 3B and Table 3).

**Table 3.** Mutation frequency of *Pm* to ENR in six strains.

Strain	Mutation Frequency ( $\times 10^{-8}$ ) ( $X \pm SD$ )
<i>PmS</i>	$0.3 \pm 0.1$
$\Delta PmS$	-
<i>PmR</i>	$6.4 \pm 2.8$
$\Delta PmR$	$3.7 \pm 1.5$
<i>PmHR</i>	$14.0 \pm 5.8$
$\Delta PmHR$	$8.2 \pm 1.6$

In order to further verify the effect of the *satP* gene deletion on *Pm* tolerance, MDK<sub>99</sub> was measured. The result showed that the speed of killing of  $\Delta PmS$ ,  $\Delta PmR$  and  $\Delta PmHR$  was faster than that of *PmS*, *PmR* and *PmHR*, which reached  $10^5$  CFU/mL. The results showed that the deletion of the *satP* gene could lead to the decrease in tolerance (Figure 4A–C).

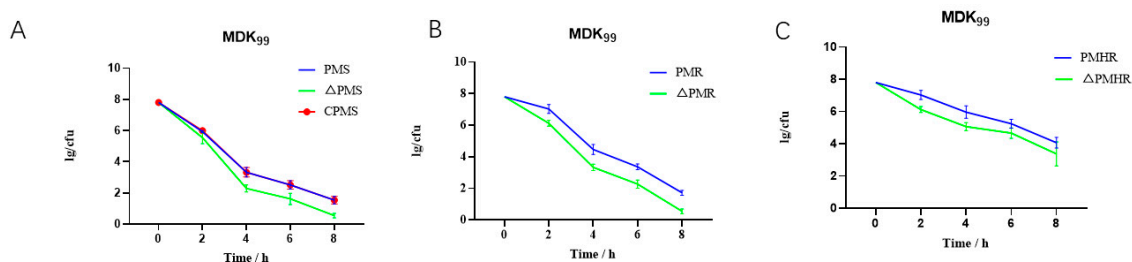


**Figure 4.** The expression level of the *satP* gene in the wild-type *S*, deletion *satP*. MDK<sub>99</sub> and survival proportions. (A–C) MDK<sub>99</sub> of *PmS*, *PmR*, *PmHR*,  $\Delta PmS$ ,  $\Delta PmR$  and  $\Delta PmHR$ .

### 3.6. Determination of Median Lethal Dose

The amount of bacteria and survival rate of 40 mice, injected intraperitoneally, were shown in Supplementary Table S6. The reasonable detection ranges were  $10^5$ – $10^7$  CFU/mL and  $10^9$ – $10^{11}$  CFU/mL. According to the data in Table S6, the LD<sub>50</sub> of *PmS* was  $1.8 \times 10^6$  CFU/mL, and the 95% confidence limit was  $1.3 \times 10^6$ – $2.5 \times 10^6$  CFU/mL, the LD<sub>50</sub> of  $\Delta PmS$  was  $7.1 \times 10^9$  CFU/mL and the 95% confidence limit was  $5.3 \times 10^9$ – $9.4 \times 10^9$  CFU/mL, the LD<sub>50</sub> of *CPmS* was  $1.8 \times 10^6$  CFU/mL and the 95% confidence limit was  $1.3 \times 10^6$ – $2.5 \times 10^6$  CFU/mL.

### 3.7. Acute Pathogenicity Protection Test in Mice

In order to evaluate the effect of the *satP* gene deletion on the infection model, we first constructed the infection model of *PmS*, *CPmS* and  $\Delta PmS$  in mice, and then injected ENR intramuscularly with a clinical therapeutic within the experimental group, and injected normal saline intramuscularly within the control group. The results are shown in Figure 5. Compared with *PmS*,  $\Delta PmS$  was more likely to be treated with ENR.

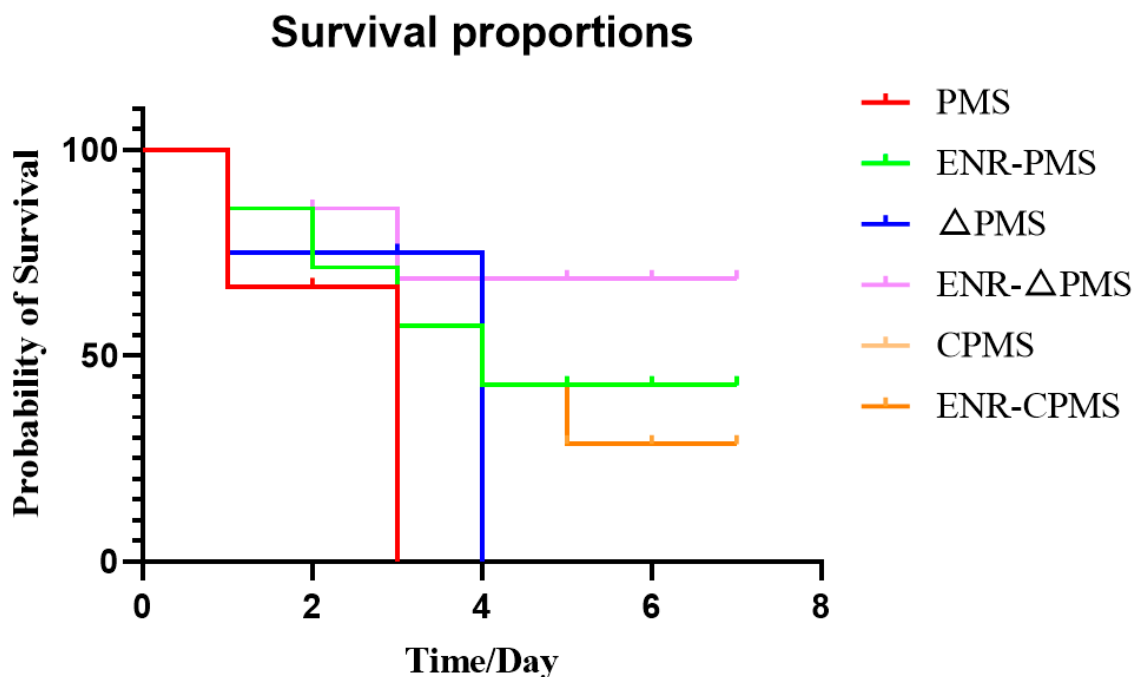


**Figure 5.** Survival rates of the mice treated with ENR infected by *PmS* and  $\Delta PmS$ .

## 4. Discussion

BRD has become one of the major diseases in the global cattle industry [36]. One of the main pathogens causing this disease is *Pm*. At present, the treatment of *Pm* mainly depends on antibiotics. However, due to the irrational use of antibiotics in clinical treatment, *Pm* is prone to drug resistance. In China, fluoroquinolones are commonly used to treat BRD infected by *Pm* [37]. In recent years, multidrug-resistant strains of *Pm* have appeared, and *Pm* has caused huge economic losses to the cattle industry worldwide. Tang et al. discovered that 93.2% of the 92 *Pm* strains were resistant to fluoroquinolones [36]. The mutation of the drug resistance target gene has a vital impact on the formation of drug resistance. Kong et al. detected the target genes in quinolone-resistant *Pm* and found that the mutation of *gyrA* and *parC* genes had a significant influence on the generation of drug resistance [37].

In this study, three strains (*PmS*, *PmR* and *PmHR*) with different resistance phenotypes in relation to fluoroquinolones were screened. We found that when the *satP* gene was deleted,  $\Delta PmS$ ,  $\Delta PmR$  and  $\Delta PmHR$  had no QRDR mutation, compared with those without deletion. The different levels of resistance between *PmHR* and *PmR* might be mediated

by other resistance mechanisms or tolerance. Relevant research has shown that antibiotic tolerance can increase the probability of antibiotic resistance [38]. With respect to the research question, we sequenced the transcriptome of three strains of bovine capsular *Pm* with different levels of drug resistance, treated by sub-inhibitory concentration, and counted the differential genes. On the basis of ensuring stable and accurate transcriptome data, we analyzed the functional annotation and metabolic pathways, and analyzed and screened the genes that might be related to the formation of drug resistance. The results showed that with the increase in drug resistance, the expression of some genes, namely *satP*, *focA*, *napF*, *glgP* and *napD*, increased significantly. The most significant difference was the *satP* gene, which was up-regulated 17 times in the drug-resistant group and 20 times in the highly drug-resistant group compared with the sensitive group. *satP* is a representative member of the AceTr family, which is preliminarily identified as a succinate acetate/proton cotransporter transmembrane protein [39]. Indrajiths et al. found that the outer membrane protein, ompk36, is an important influencing factor of cefoxitin and carbapenem resistance [40]. Yamamoto et al. found that the membrane protein mmp15 has an effect on the resistance of clofazimine and is also related to the tolerance of a variety of antibiotics [41]. Lu et al. studied the function of membrane channel protein, *lamB*, and found that it can produce antibiotic resistance by reducing the pressure of protein translation and DNA replication. In order to further detect antibiotic resistance, the *lamB* gene was knocked out and was found to increase antibiotic resistance by reducing the activity of metabolic pathways such as the tricarboxylic acid (TCA) cycle, pentose phosphate pathway and glycolysis/gluconeogenesis. By comparing the function of the wild-type strain and deletion strain after ciprofloxacin treatment, it was found that the down-regulation of the *lamB* gene can increase the resistance of bacteria to antibiotics [42].

Based on the research background of the *satP* gene, in order to further confirm the function of the *satP* gene, we constructed the gene deletion strain of a sensitive strain and drug-resistant strain. The results showed that the tolerance of *satP* decreased after the deletion of the *satP* gene. Safi et al. have pointed out that when antibiotics act on bacteria, antibiotic tolerance first appears. When antibiotics continue to act, antibiotic tolerance will aggravate the generation of drug resistance. Compared with the life cycle of drug resistance phenotype, antibiotic tolerance is a temporary state. Timely release of antibiotics can restore its tolerance, so the tolerance is reversible [43]. Repeated exposure will maintain the tolerance [44], which reaffirms the foundation for functional studies. During the research of this gene in *Pm*, Westfall et al. studied the mechanism of MRSA tolerance by using triclosan, an antibacterial agent synthesized by fatty acids, to induce the change of MRSA tolerance. MDK<sub>99</sub> and the agar diffusion method were used to detect its tolerance. The results showed that triclosan increased the tolerance of *LL* to bactericidal antibiotics by 10,000 times, and reduced the efficacy of antibiotics by 100 times. Genetic analysis showed that the antibiotic tolerance mediated by triclosan needs the cooperation of ppGpp [33]. However, until now, there was no report about *satP*-gene-mediated tolerance; other membrane transporters have been confirmed to be involved in the formation of tolerance. Poudyal et al. found a *MerR*-type transcriptional activator, which can activate the *BrlR* target encoding ABC transport system gene and affect the drug tolerance of bacteria [45]. One of the main stress responses of almost all bacteria depends on the rapid accumulation of ppGpp, an alarmone. Many scholars have found that ppGpp has a great impact on bacterial tolerance. Recently, Ronneau et al. and others have studied ppGpp and found that the concentration of ppGpp is determined by a highly conserved and widely distributed protein family, and the family is known as RelA-Spot Homologs (RSH). Recent studies have found that RSH can affect not only the tolerance of bacteria, but also the drug resistance and virulence of bacteria [46].

One unanticipated finding was that the virulence of the *satP* gene deletion strain was several times lower than that of the wild-type strain, and we found that the treatment rate of the mice infected with  $\Delta PmS$  was higher. This finding broadly supports the work of other studies in this area which links tolerance with virulence [47]. However, there are also some reports contrary to this study. Ma et al. knocked out the *MazEF* gene of three

strains of bacteria and found that the tolerance of the deletion strain was decreased and the virulence was enhanced, compared with the wild-type strain [48]. These findings may help us understand the relationship between drug resistance and adaptive compensation. This finding has important implications for developing inhibitors. Nevertheless, there are still many unanswered questions regarding whether *satP* can be used as a target of drug resistance inhibitors and how effective it could be in clinical application. More attention should be paid to studying *satP* and its inhibitors.

## 5. Conclusions

In this study, based on the transcriptome sequence of three strains of *Pm*, the *satP* gene was obtained, of which the expression was significantly up-regulated with the increase in drug resistance. Through the study of the formation of the *satP* gene of drug resistance, the deletion of the *satP* gene in *Pm* can lead to a faster growth rate, longer development time of drug resistance and reduced tolerance. In addition, due to the deletion of the *satP* gene, its virulence was 400 times reduced than in the wild-type strain. The results indicated that *satP* might be the target of ENR resistance inhibitors.

**Supplementary Materials:** The following supporting information can be downloaded at: <https://www.mdpi.com/article/10.3390/vetsci10040257/s1>, Figure S1. Identification of *Pm*; Figure S2. The density of FPKM; Figure S3. Histogram of differential gene between groups; Figure S4. DEGs of biological process, cellular component and molecular function GO terms; Figure S5. The enrichment bubble map of KEGG; Table S1. Primer sequence; Table S2. The quality analysis of total RNA in *Pm*; Table S3. Statistical results of trimmed reads mapping with reference genome; Table S4. The Statistics of functional annotation; Table S5. The results of top GO; Table S6. LD<sub>50</sub> test results of *PmS* and  $\Delta PmS$ .

**Author Contributions:** Conceptualization, L.-C.K. and H.-X.M.; Data curation, Y.Q.; Funding acquisition, L.-C.K. and H.-X.M.; Investigation, X.-Y.L.; Methodology, J.-Z.X.; Resources, Y.-X.X.; Software, X.-S.L. and Y.Q.; Supervision, L.-C.K. and H.-X.M.; Validation, G.-Y.X.; Writing—original draft, X.-S.L. and Y.Q.; Writing—review and editing, I.M. All authors have read and agreed to the published version of the manuscript.

**Funding:** This work was supported by the National Natural Science Foundation of China (Grants: 31872519), and the Jilin Natural Science Foundation (20190201294JC).

**Institutional Review Board Statement:** The study was conducted according to the guidelines of the Declaration of Helsinki, and all of the experimental procedures with mice were performed at the Experimental Animal Center, under protocol number JLAU20210423001. The experiments were conducted under the supervision of the Experimental Animal Welfare and Ethics Committee of the Jilin Agricultural University. All methods were performed in accordance with the relevant guidelines and regulations.

**Informed Consent Statement:** Not applicable.

**Data Availability Statement:** The transcriptome data of the bacteria under study have been uploaded to NCBI GenBank, with the admission number 8172276. The data set generated and analyzed during this study can be obtained from the corresponding authors upon reasonable requirements.

**Acknowledgments:** We thank all the participants for their advice and support during this study.

**Conflicts of Interest:** The authors declare no conflict of interest.

## References

1. Townsend, K.M.; Boyce, J.D.; Chung, J.Y.; Frost, A.J.; Adler, B. Genetic organization of *Pasteurella multocida* cap Loci and development of a multiplex capsular PCR typing system. *J. Clin. Microbiol.* **2001**, *39*, 924–929. [[CrossRef](#)] [[PubMed](#)]
2. Christenson, E.S.; Ahmed, H.M.; Durand, C.M. *Pasteurella multocida* infection in solid organ transplantation. *Lancet Infect. Dis.* **2015**, *15*, 235–240. [[CrossRef](#)]
3. Zhao, G.; He, H.; Wang, H. Use of a recombinase polymerase amplification commercial kit for rapid visual detection of *Pasteurella multocida*. *BMC Vet. Res.* **2019**, *15*, 154. [[CrossRef](#)] [[PubMed](#)]

4. Stanford, K.; Zaheer, R.; Klima, C.; McAllister, T.; Peters, D.; Niu, Y.D.; Ralston, B. Antimicrobial resistance in members of the bacterial bovine respiratory disease complex isolated from lung tissue of cattle mortalities managed with or without the use of antimicrobials. *Microorganisms* **2020**, *8*, 288. [[CrossRef](#)] [[PubMed](#)]
5. Elsayed, M.; Eldsouky, S.M.; Roshdy, T.; Said, L.; Thabet, N.; Allam, T.; Mohammed, A.B.A.; Nasr, G.M.; Basiouny, M.S.M.; Akl, B.A.; et al. Virulence determinants and antimicrobial profiles of *Pasteurella multocida* isolated from cattle and humans in Egypt. *Antibiotics* **2021**, *10*, 480. [[CrossRef](#)] [[PubMed](#)]
6. Peng, Z.; Wang, H.; Liang, W.; Chen, Y.; Tang, X.; Chen, H.; Wu, B. A capsule/lipopolysaccharide/MLST genotype D/L6/ST11 of *Pasteurella multocida* is likely to be strongly associated with swine respiratory disease in China. *Arch. Microbiol.* **2018**, *200*, 107–118. [[CrossRef](#)]
7. Jourquin, S.; Lowie, T.; Debruyne, F.; Chantillon, L.; Vereecke, N.; Boyen, F.; Boone, R.; Bokma, J.; Pardon, B. Dynamics of subclinical pneumonia in male dairy calves in relation to antimicrobial therapy and production outcomes. *J. Dairy Sci.* **2023**, *106*, 676–689. [[CrossRef](#)]
8. Becker, J.; Perreten, V.; Schüpbach-Regula, G.; Stucki, D.; Steiner, A.; Meylan, M. Associations of antimicrobial use with antimicrobial susceptibility at the calf level in bacteria isolated from the respiratory and digestive tracts of veal calves before slaughter. *J. Antimicrob. Chemother.* **2022**, *77*, 2859–2866. [[CrossRef](#)]
9. Wang, Z.; Kong, L.C.; Jia, B.Y.; Liu, S.M.; Jiang, X.Y.; Ma, H.X. Aminoglycoside susceptibility of *Pasteurella multocida* isolates from bovine respiratory infections in China and mutations in ribosomal protein S5 associated with high-level induced spectinomycin resistance. *J. Vet. Med. Sci.* **2017**, *79*, 1678–1681. [[CrossRef](#)]
10. Kong, L.C.; Wang, Z.; Wang, Y.M.; Dong, W.L.; Jia, B.Y.; Gao, D.; Jiang, X.Y.; Ma, H.X. Antimicrobial susceptibility and molecular typing of *Pasteurella multocida* isolated from six provinces in China. *Trop. Anim. Health Prod.* **2019**, *51*, 987–992. [[CrossRef](#)]
11. Khamesipour, F.; Momtaz, H.; Azhdary Mamoreh, M. Occurrence of virulence factors and antimicrobial resistance in *Pasteurella multocida* strains isolated from slaughter cattle in Iran. *Front. Microbiol.* **2014**, *5*, 536. [[CrossRef](#)] [[PubMed](#)]
12. Coetzee, J.F.; Magstadt, D.R.; Sidhu, P.K.; Follett, L.; Schuler, A.M.; Krull, A.C.; Cooper, V.L.; Engelken, T.J.; Kleinhenz, M.D.; O'Connor, A.M. Association between antimicrobial drug class for treatment and retreatment of bovine respiratory disease (BRD) and frequency of resistant BRD pathogen isolation from veterinary diagnostic laboratory samples. *PLoS ONE* **2019**, *14*, e0219104. [[CrossRef](#)] [[PubMed](#)]
13. Zhu, D.; Yuan, D.; Wang, M.; Jia, R.; Chen, S.; Liu, M.; Zhao, X.; Yang, Q.; Wu, Y.; Zhang, S.; et al. Emergence of a multidrug-resistant hypervirulent *Pasteurella multocida* ST342 strain with a floR-carrying plasmid. *J. Glob. Antimicrob. Resist.* **2020**, *20*, 348–350. [[CrossRef](#)] [[PubMed](#)]
14. Timsit, E.; Hallewell, J.; Booker, C.; Tison, N.; Amat, S.; Alexander, T.W. Prevalence and antimicrobial susceptibility of *Mannheimia haemolytica*, *Pasteurella multocida*, and *Histophilus somni* isolated from the lower respiratory tract of healthy feedlot cattle and those diagnosed with bovine respiratory disease. *Vet. Microbiol.* **2017**, *208*, 118–125. [[CrossRef](#)] [[PubMed](#)]
15. Blondeau, J.M.; Fitch, S.D. Mutant prevention and minimum inhibitory concentration drug values for enrofloxacin, ceftiofur, florfenicol, tilmicosin and tulathromycin tested against swine pathogens *Actinobacillus pleuropneumoniae*, *Pasteurella multocida* and *Streptococcus suis*. *PLoS ONE* **2019**, *14*, e0210154. [[CrossRef](#)]
16. Balaje, R.M.; Sidhu, P.K.; Kaur, G.; Rampal, S. Mutant prevention concentration and PK-PD relationships of enrofloxacin for *Pasteurella multocida* in buffalo calves. *Res. Vet. Sci.* **2013**, *95*, 1114–1124. [[CrossRef](#)]
17. Michael, G.B.; Kadlec, K.; Sweeney, M.T.; Brzuszkiewicz, E.; Liesegang, H.; Daniel, R.; Murray, R.W.; Watts, J.L.; Schwarz, S. ICEPmu1, an integrative conjugative element (ICE) of *Pasteurella multocida*: Analysis of the regions that comprise 12 antimicrobial resistance genes. *J. Antimicrob. Chemother.* **2012**, *67*, 84–90. [[CrossRef](#)]
18. Hooper, D.C.; Jacoby, G.A. Mechanisms of drug resistance: Quinolone resistance. *Ann. N. Y. Acad. Sci.* **2015**, *1354*, 12–31. [[CrossRef](#)]
19. Cárdenas, M.; Barbé, J.; Llagostera, M.; Miró, E.; Navarro, F.; Mirelis, B.; Prats, G.; Badiola, I. Quinolone resistance-determining regions of *gyrA* and *parC* in *Pasteurella multocida* strains with different levels of nalidixic acid resistance. *Antimicrob. Agents Chemother.* **2001**, *45*, 990–991. [[CrossRef](#)]
20. Fuzi, M.; Szabo, D.; Csercsik, R. Double-serine fluoroquinolone resistance mutations advance major international clones and lineages of various multi-drug resistant bacteria. *Front. Microbiol.* **2017**, *8*, 2261. [[CrossRef](#)]
21. Kong, L.C.; Gao, D.; Gao, Y.H.; Liu, S.M.; Ma, H.X. Fluoroquinolone resistance mechanism of clinical isolates and selected mutants of *Pasteurella multocida* from bovine respiratory disease in China. *J. Vet. Med. Sci.* **2014**, *76*, 1655–1657. [[CrossRef](#)] [[PubMed](#)]
22. Rosas, N.C.; Lithgow, T. Targeting bacterial outer-membrane remodelling to impact antimicrobial drug resistance. *Trends Microbiol.* **2022**, *30*, 544–552. [[CrossRef](#)]
23. Rodrigues, I.C.; Rodrigues, S.C.; Duarte, F.V.; Costa, P.M.D.; Costa, P.M.D. The role of outer membrane proteins in UPEC antimicrobial resistance: A systematic review. *Membranes* **2022**, *12*, 981. [[CrossRef](#)] [[PubMed](#)]
24. Rattanapanadda, P.; Kuo, H.C.; Chang, S.K.; Tell, L.A.; Shia, W.Y.; Chou, C.C. Effect of carbonyl cyanide chlorophenylhydrazone on intrabacterial concentration and antimicrobial activity of amphenicols against swine resistant *Actinobacillus pleuropneumoniae* and *Pasteurella multocida*. *Vet. Res. Commun.* **2022**, *46*, 903–916. [[CrossRef](#)]
25. Nishino, K.; Yamasaki, S.; Nakashima, R.; Zwama, M.; Hayashi-Nishino, M. Function and inhibitory mechanisms of multidrug efflux pumps. *Front. Microbiol.* **2021**, *12*, 737288. [[CrossRef](#)] [[PubMed](#)]

26. Li, X.Z.; Plésiat, P.; Nikaido, H. The challenge of efflux-mediated antibiotic resistance in Gram-negative bacteria. *Clin. Microbiol. Rev.* **2015**, *28*, 337–418. [[CrossRef](#)]
27. Shin, B.; Park, C.; Park, W. Stress responses linked to antimicrobial resistance in *Acinetobacter* species. *Appl. Microbiol. Biotechnol.* **2020**, *104*, 1423–1435. [[CrossRef](#)]
28. Cao, L.; Wang, J.; Sun, L.; Kong, Z.; Wu, Q.; Wang, Z. Transcriptional analysis reveals the relativity of acid tolerance and antimicrobial peptide resistance of *Salmonella*. *Microb. Pathog.* **2019**, *136*, 103701. [[CrossRef](#)]
29. Lewis, K.; Shan, Y. Why tolerance invites resistance. *Science* **2017**, *355*, 796. [[CrossRef](#)]
30. Beaber, J.W.; Hochhut, B.; Waldor, M.K. SOS response promotes horizontal dissemination of antibiotic resistance genes. *Nature* **2004**, *427*, 72–74. [[CrossRef](#)]
31. Alam, M.K.; Alhazmi, A.; DeCoteau, J.F.; Luo, Y.; Geyer, C.R. RecA inhibitors potentiate antibiotic activity and block evolution of antibiotic resistance. *Cell Chem. Biol.* **2016**, *23*, 381–391. [[CrossRef](#)] [[PubMed](#)]
32. Thomas, E.; Grandemange, E.; Pommier, P.; Wessel-Robert, S.; Davot, J.L. Field evaluation of efficacy and tolerance of a 2% marbofloxacin injectable solution for the treatment of respiratory disease in fattening pigs. *Vet. Q.* **2000**, *22*, 131–135. [[CrossRef](#)] [[PubMed](#)]
33. Westfall, C.; Flores-Mireles, A.L.; Robinson, J.I.; Lynch, A.J.L.; Hultgren, S.; Henderson, J.P.; Levin, P.A. The widely used antimicrobial triclosan induces high levels of antibiotic tolerance in vitro and reduces antibiotic efficacy up to 100-fold in vivo. *Antimicrob. Agents Chemother.* **2019**, *63*, e02312-18. [[CrossRef](#)] [[PubMed](#)]
34. Cirz, R.T.; Chin, J.K.; Andes, D.R.; de Crécy-Lagard, V.; Craig, W.A.; Romesberg, F.E. Inhibition of mutation and combating the evolution of antibiotic resistance. *PLoS Biol.* **2005**, *3*, e176. [[CrossRef](#)]
35. Zuluaga, A.F.; Salazar, B.E.; Rodriguez, C.A.; Zapata, A.X.; Agudelo, M.; Vesga, O. Neutropenia induced in outbred mice by a simplified low-dose cyclophosphamide regimen: Characterization and applicability to diverse experimental models of infectious diseases. *BMC Infect. Dis.* **2006**, *6*, 55. [[CrossRef](#)]
36. Tang, X.; Zhao, Z.; Hu, J.; Wu, B.; Cai, X.; He, Q.; Chen, H. Isolation, antimicrobial resistance, and virulence genes of *Pasteurella multocida* strains from swine in China. *J. Clin. Microbiol.* **2009**, *47*, 951–958. [[CrossRef](#)]
37. Kong, L.C.; Gao, D.; Jia, B.Y.; Wang, Z.; Gao, Y.H.; Pei, Z.H.; Liu, S.M.; Xin, J.Q.; Ma, H.X. Antimicrobial susceptibility and molecular characterization of macrolide resistance of *Mycoplasma bovis* isolates from multiple provinces in China. *J. Vet. Med. Sci.* **2016**, *78*, 293–296. [[CrossRef](#)]
38. Sun, P.; Li, J.; Zhang, X.; Guan, Z.; Xiao, Q.; Zhao, C.; Song, M.; Zhou, Y.; Mou, L.; Ke, M.; et al. Crystal structure of the bacterial acetate transporter SatP reveals that it forms a hexameric channel. *J. Biol. Chem.* **2018**, *293*, 19492–19500. [[CrossRef](#)]
39. Indrajith, S.; Mukhopadhyay, A.K.; Chowdhury, G.; Farraj, D.A.A.; Alkufeidy, R.M.; Natesan, S.; Meghanathan, V.; Gopal, S.; Muthupandian, S. Molecular insights of carbapenem resistance *Klebsiella pneumoniae* isolates with focus on multidrug resistance from clinical samples. *J. Infect. Public Health* **2021**, *14*, 131–138. [[CrossRef](#)]
40. Yamamoto, K.; Nakata, N.; Mukai, T.; Kawagishi, I.; Ato, M. Coexpression of MmpS5 and MmpL5 contributes to both efflux transporter MmpL5 trimerization and drug resistance in *Mycobacterium tuberculosis*. *mSphere* **2021**, *6*. [[CrossRef](#)]
41. Li, W.; Wang, G.; Zhang, S.; Fu, Y.; Jiang, Y.; Yang, X.; Lin, X. An integrated quantitative proteomic and metabolomics approach to reveal the negative regulation mechanism of LamB in antibiotics resistance. *J. Proteom.* **2019**, *194*, 148–159. [[CrossRef](#)] [[PubMed](#)]
42. Safi, H.; Gopal, P.; Lingaraju, S.; Ma, S.; Levine, C.; Dartois, V.; Yee, M.; Li, L.; Blanc, L.; Ho Liang, H.P.; et al. Phase variation in *Mycobacterium tuberculosis* *glpK* produces transiently heritable drug tolerance. *Proc. Natl. Acad. Sci. USA* **2019**, *116*, 19665–19674. [[CrossRef](#)] [[PubMed](#)]
43. Petes, C.; Mintsopoulos, V.; Finnen, R.L.; Banfield, B.W.; Gee, K. The effects of CD14 and IL-27 on induction of endotoxin tolerance in human monocytes and macrophages. *J. Biol. Chem.* **2018**, *293*, 17631–17645. [[CrossRef](#)]
44. Poudyal, B.; Sauer, K. The ABC of Biofilm Drug Tolerance: The MerR-like regulator BrIR is an activator of ABC transport systems, with PA1874-77 contributing to the tolerance of *Pseudomonas aeruginosa* biofilms to tobramycin. *Antimicrob. Agents Chemother.* **2018**, *62*. [[CrossRef](#)]
45. Ronneau, S.; Hallez, R. Make and break the alarmone: Regulation of (p)ppGpp synthetase/hydrolase enzymes in bacteria. *FEMS Microbiol. Rev.* **2019**, *43*, 389–400. [[CrossRef](#)]
46. Niu, Y.; Wang, K.; Zheng, S.; Wang, Y.; Ren, Q.; Li, H.; Ding, L.; Li, W.; Zhang, L. Antibacterial effect of caffeic acid phenethyl ester on *Cariogenic Bacteria* and *Streptococcus mutans* biofilms. *Antimicrob. Agents Chemother.* **2020**, *64*, e00251-2. [[CrossRef](#)] [[PubMed](#)]
47. Zhan, L.; Zhang, J.; Zhao, B.; Li, X.; Zhang, X.; Hu, R.; Elken, E.M.; Kong, L.; Gao, Y. Genomic and transcriptomic analysis of bovine *Pasteurella multocida* serogroup a strain reveals insights into virulence attenuation. *Front. Vet. Sci.* **2021**, *8*, 765495. [[CrossRef](#)]
48. Ma, D.; Mandell, J.B.; Donegan, N.P.; Cheung, A.L.; Ma, W.; Rothenberger, S.; Shanks, R.M.Q.; Richardson, A.R.; Urish, K.L. The Toxin-antitoxin MazEF drives *Staphylococcus aureus* biofilm formation, antibiotic tolerance, and chronic infection. *mBio* **2019**, *10*. [[CrossRef](#)]

**Disclaimer/Publisher's Note:** The statements, opinions and data contained in all publications are solely those of the individual author(s) and contributor(s) and not of MDPI and/or the editor(s). MDPI and/or the editor(s) disclaim responsibility for any injury to people or property resulting from any ideas, methods, instructions or products referred to in the content.